FACTA UNIVERSITATIS
Series: **Architecture and Civil Engineering** Vol. 6, N° 2, 2008, pp. 155 - 164
DOI:10.2298/FUACE0802155H

VIBRATIONS OF CRACKED REINFORCED AND PRESTRESSED CONCRETE BEAMS

UDC 624.072.2:624.012.45/.46:534.17(045)=111

Zsolt Huszár

Budapest University of Technology and Economics Department of Structures
1111 Budapest Bertalan Lajos utca 2
Email: huszar@vbt.bme.hu

Abstract. *The dynamic behaviour of bent reinforced concrete beams in elastic range is significantly influenced by cracks caused by former loads. Considering this fact a more accurate calculation of the eigenfrequencies of the beams is available. Experiments have shown that the features of vibration differ from the results obtained by the well-known linear model, if cracked zones exist. The cause of this phenomenon is that the bending rigidity of the cross-sections in the cracked range depends on the sign of the actual bending moment. Therefore the vibration shows non-linear characteristics in the elastic range as well.*
The dynamic behaviour of bent prestressed concrete beams is similar. The dynamic characteristics of prestressed beams besides cracks is influenced also by the intensity and eccentricity of the axial force.
For a detailed investigation of the problem, experiments and non-linear analysis were performed. On the basis of these the virtual eigenfrequencies of the non-linear vibrations were determined.

Key words: *Vibrations, Prestressed Concrete, Beam*

1. VIBRATIONS OF CRACKED REINFORCED CONCRETE BEAMS

1.1 Introduction

The dynamic behaviour of the cracked reinforced concrete beam was examined by experiments [1] in the Laboratory of Reinforced Concrete Structures at the Technical University of Budapest.

First, in that experiment in the middle third part of the examined reinforced concrete beam cracks were induced by so large *P* forces, where the bending moment exceeded the cracking moment (Fig. 1).

Received March 03, 2008

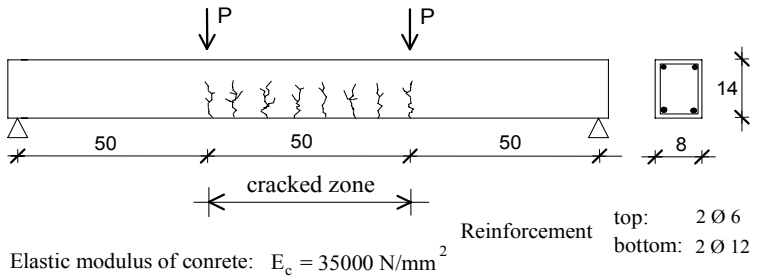

Fig. 1 Model used at the experiments

After removing the static P forces, the beam was brought into vibration with an exterior impact load, by a rubber hammer blow. According to the spectral decomposition of the time-deflection series, the first eigenfrequency resulted in 98 Hz. In addition a secondary peak has also appeared at 89 Hz. The calculations of non-linear examinations showed good coincidence with the experiments.

If the beam will be considered free from cracks, then the eigenfrequencies can be determined in an elementary way with the well-known formula (1):

$$f_n = \frac{\pi}{2}\left(\frac{n}{\ell}\right)^2 \sqrt{\frac{EI}{m}} \tag{1}$$

The first three eigenfrequencies of the uncracked beam are: $f_1 = 109$ Hz, $f_2 = 436$ Hz, $f_3 = 981$ Hz. According to expectations, the first eigenfrequency of the uncracked beam is larger than the result shown in the experiment. The cause of this difference is that during the vibration the bending rigidity of the cross-sections in the cracked range is not constant. It depends, whether cracks close or open. If cracks were caused by positive moments, the flexural stiffness of the beam in the cracked zones can be described with the formula below:

$$EI_i = \begin{cases} E_c I_{i,I} & \text{if} \quad M_i < 0 \\ E_c I_{i,II} & \text{if} \quad M_i \geq 0 \end{cases} \tag{2}$$

where: $I_{i,I}$ is the moment of inertia of the uncracked section and $I_{i,II}$ is that of the cracked section.

So the vibration shows non-linear characteristics in the elastic range as well. In this case only virtual eigenfrequencies could be investigated.

1.2 The computation method

The dynamic behaviour of the cracked beam in the elastic range, can be described by the well-known differential equation with varying coefficients [2]:

$$\frac{\partial^2}{\partial x^2}\left(EI(x)\frac{\partial^2 w}{\partial x^2} + c_s I(x)\frac{\partial^3 w}{\partial x^2 \partial t} \right) + c\frac{\partial w}{\partial t} + m(x)\frac{\partial^2 w}{\partial t^2} = q(x,t) \tag{3}$$

where: x is the coordinate in axial direction, $w(x,t)$ is the displacement perpendicular to the axis of the beam, $EI(x)$ is the flexural stiffness, c_s and c are the damping coefficients, $m(x)$ is the specific mass per unit length and $q(x,t)$ is the external distributed load.

The solution of the non-linear vibration problem needs discretising in time and in space. The discretising in the axial direction was made with the difference method. The beam model (Fig. 1) was in the calculation divided in 18 equal parts along the longitudinal axis. For the description of the relationship between the bending moment and the deflection (4), as well as of the relationship between the loading and the bending moment (5), the difference operators were used:

$$M_i = -EI\frac{\partial^2 w}{\partial x^2} \approx -\frac{EI}{\Delta\ell^2}(w_{i-1} - 2w_i + w_{i+1}) \tag{4}$$

$$q_i = -\frac{\partial^2 M}{\partial x^2} \approx -\frac{1}{\Delta\ell^2}(M_{i-1} - 2M_i + M_{i+1}) \tag{5}$$

where: $\Delta\ell$ is the distance of the dividing points.

Making use of Eq. (3), (4), (5), and neglecting damping, the equation of motion for the discrete system, Eq. (6) can be assembled. In the equation below the $\{u\}$ vector contains the w_i vertical displacements of the nodal points [3].

$$[K]\{u\} + [M]\{\ddot{u}\} = \{F(t)\} \tag{6}$$

The equation of the motion (6) contains already the boundary conditions, the hinged supports at both ends of the beam. In the case of constant flexural stiffness in time, the modal solution of the vibration problem can be obtained by the homogeneous form of Eq. (6).

Considering the non-linear properties, due to the relation (2), makes it necessary the discretising in time, by applying a time-step algorithm. For that purpose Wilson's method was used [4].

On basis of the above method a MATLAB program was elaborated.

1.3 Numerical investigations

With the MATLAB program there were numerical simulations carried out on the linear and non-linear computing model of the beam in Fig. 1. For the sake of a detailed analysis of the dynamic behaviour of the beam the non-linear analysis was performed both with and without considering the gravitational forces.

1.3.1 Examinations on the linear model

The linear vibration problem can be solved assuming a constant flexural stiffness in time. This makes possible the estimation of the virtual eigenfrequencies of the beam in Fig. 1, by giving upper and lower boundaries. A lower boundary can be obtained, if in the cracked region the smaller flexural stiffness EI_{II} is substituted and regarded as constant in time. This would be the model of a beam in which cracks are produced in the middle third region at both faces by positive and negative moments (weakened beam). To obtain the upper boundary for the investigated eigenfrequencies, the greater flexural stiffness EI_I

should be applied in the middle part. With this constant EI_I an uncracked beam is modelled. In the undamped case, the eigenfrequencies can be derived, by solving the eigenvalue problem, coming from Eq. (6):

$$([K]-\omega_i^2[M])\{u_i\} \tag{7}$$

With making use of the computing model the first three eigenfrequencies of the uncracked beam and of the weakened beam were determined. The results are shown in Table 2.

1.3.2 *Examinations on the non-linear model, neglecting the gravitational forces*

Considering the periodically varying flexural stiffness in time (2), on the non-linear model a free vibration problem was examined. For this purpose an impact load was modelled in the section x = ℓ/3, as follows:

$$F(t,x)=\begin{cases}F_0 & \text{if} \quad t \le \Delta t \quad \text{and} \quad x=\ell/3 \\ 0 & \text{if} \quad t > \Delta t\end{cases} \tag{8}$$

This corresponds essentially to the experiment carried out on the beam presented in Fig. 1.

The virtual eigenfrequencies of this quasi-periodical motion was determined by discrete Fourier transformation [5] of the time-deflection data series. On Fig. 2 it can be seen that the spectrum range 0-500 Hz contains the first two eigenfrequencies. The third eigenfrequency did not appear, because mode shape 3 has a nodal point in the cross-section of the impact load action. The first virtual eigenfrequency according to Fig. 2 was 96 Hz. It means that the non-linear calculation and the experiment have shown a good coincidence.

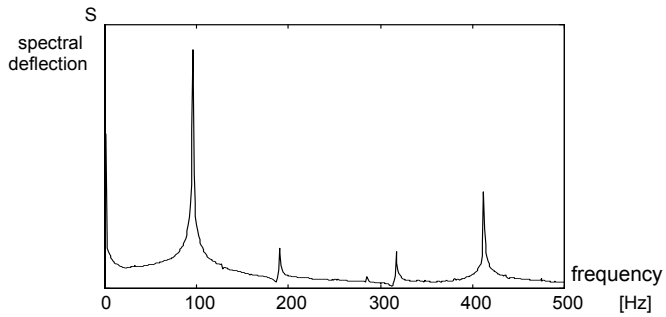

Fig. 2 The spectral decomposition of the time-deflection

1.3.3 Examinations on the non-linear model considering the gravitational forces

The computation model in Chapter 1.3.2 does not show the spontaneous separation of the first eigenfrequency, namely the existence of the secondary peak in the experiment. To the first eigenmode belongs only one virtual eigenfrequency (Fig. 2).

However, when taking into consideration the self-weight, the situation changes. Due to the self-weight cracks open in the middle region, already in the static condition. Thus the stepwise change of the flexural stiffness is the following:

$$EI_i = \begin{cases} E_c I_{i,I} & \text{if} \quad M_{dyn,i} + M_{stat,i} < 0 \\ E_c I_{i,II} & \text{if} \quad M_{dyn,i} + M_{stat,i} \geq 0 \end{cases} \tag{9}$$

This means a shifting of the base line compared with relation (2). In case of a sufficiently large starting impulse, in the first part of the observed vibration the cracks still close in each period when negative resultant moment arises. In the second part of the time-interval as dynamic moment becomes smaller due to damping, the cracks will not close. The double peak can appear in the spectrum if there is an appropriate relation among the starting impulse, the self-weight and the damping.

Taking the self-weight into assumption, the vibration spectrum was produced by the Wilson type time-step integral, which is shown in Fig. 3.

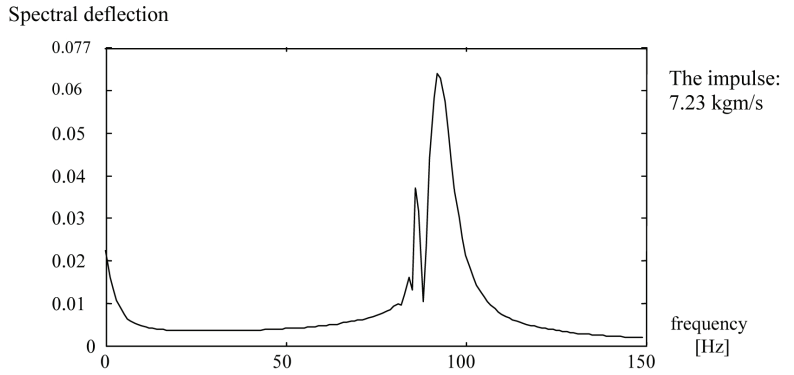

Fig. 3 Double peak in the spectrum of the beam model

The first virtual eigenfrequencies, according to the spectrum, have the values in 87 Hz and 94 Hz. In the experiment these frequencies have been found to be 89 Hz, and 98 Hz.

The main peak (94 Hz) derived from this non-linear analysis with self-weight is a little smaller than the 96 Hz, obtained from the previous non-linear calculation without self-weight. That is because of the self-weight, the smaller flexural stiffness of the cracked section is valid for a little longer segment of the periods than before. The secondary peak represents a larger frequency than the lower boundary 85 Hz, obtained from the linear calculation of the weakened beam.

The double peak here does not mean two frequencies of a quasi-resonant state. The examined interval of the vibration is divided into two parts due to damping. In the first part of the vibration the cracks still close, but in the second part they do not. In case of forced harmonic vibration of continuously increasing frequency, only one quasi-resonant state can be found in the first mode.

1.4 Comparison of the experiments and the calculations

The results of the experiments and the calculations are summarized in Table 1. The calculations of non-linear examinations show good coincidence with the experiments.

The double peak, which appeared in the spectrum of experiments, can be obtained also by numerical simulation.

Table 1 The results of the experiments and the calculations

Experiments and calculations	f_1 [Hz]	f_2 [Hz]
Experiment, real beam	89, 98	
Linear computation, uncracked beam	109	436
Linear computation, weakened beam	85	397
Non-linear computation, without self-weight	96	414
Non-linear computation, with self-weight	87, 94	

In general cases, when considering different ratios of static loads (containing the self-weight) and dynamic loads, the virtual eigenfrequency falls in an interval determined by two extreme cases:

A. When large self-weight or static forces are coupled with small dynamic loads, the vibration of the beam is similar to the behaviour of the weakened beam in Chapter 1.3.1.

B. When the static loads are relatively small compared with the dynamic loads, the vibration of the beam is similar to the case shown in Chapter 1.3.2.

2. VIBRATIONS OF CRACKED PRESTRESSED CONCRETE BEAMS

2.1 Bending stiffness in the cracked region

The bent and cracked prestressed concrete beam can also be considered as a member subjected to eccentric compression. The curvature of the cracked concrete section under eccentric compression should be calculated in a different manner as in the case of the pure bending [4]. The position of the neutral axis depends on the eccentricity of the normal force and in this way influences the bending stiffness of the section (Fig. 4).

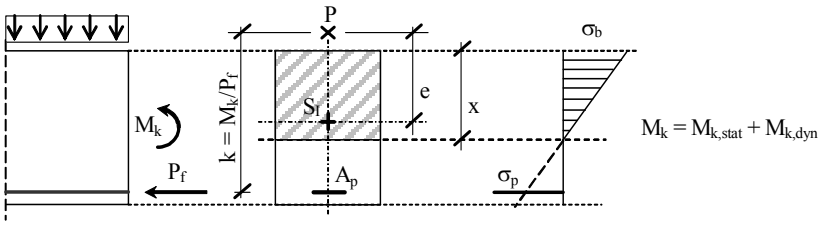

Fig. 4 Prestressed, cracked section subjected to bending

In Fig. 4 the M_k is the moment due to external loads. In case of vibration it is the sum of the static and dynamic moment. The M_k moment and the P_f tension force are together equivalent with the P force in Fig. 4. The bending stiffness of the section under eccentric compression can be defined with the aid of curvature's concept. [6]. The g curvature of the section:

$$g = \frac{\varepsilon_b}{x} = \frac{\sigma_b}{E_b x} = \frac{M}{E_b I}, \tag{10}$$

where: σ_b is the concrete stress, ε_b is the concrete strain in the extreme fibre; E_bI is the bending stiffness in which I is the wanted moment of inertia.

The moment around the S_I horizontal centroidal axis of the uncracked section due to the external moment and the P_f tension force (Fig. 4), can be expressed as:

$$M = M_k - M_f = P_f k - P_f (k - e) = P_f e = Pe\,. \tag{11}$$

From the equilibrium equation of the forces yields:

$$\sigma_b = \frac{P_f}{S_d} x\,, \tag{12}$$

where: S_d is the static moment of the section's active part to the neutral axis. Substituting (11) and (12) into (10), the moment of inertia can be obtained:

$$I = I_g = S_d e\,. \tag{13}$$

The I_g section property is called moment of inertia of curvature [4]. In this way the I_g is the function of the eccentricity of the normal force. If the resultant normal force is acting within the core, the cracks close and (13) results the $I_{i,I}$ moment of inertia (upper boundary) of the uncracked section. If the eccentricity of the resultant normal force is $e \to \infty$ then the section is subjected to the pure bending and (13) results the $I_{i,II}$ moment of inertia (lower boundary) of the cracked section.

2.2 Numeric modelling of a prestressed beam

Making use of the calculation model detailed in Chapter 1 and 2.1, the vibration of the cracked, prestressed beam was examined (Fig. 5). For the purpose of the numeric simulation a MATLAB program was prepared.

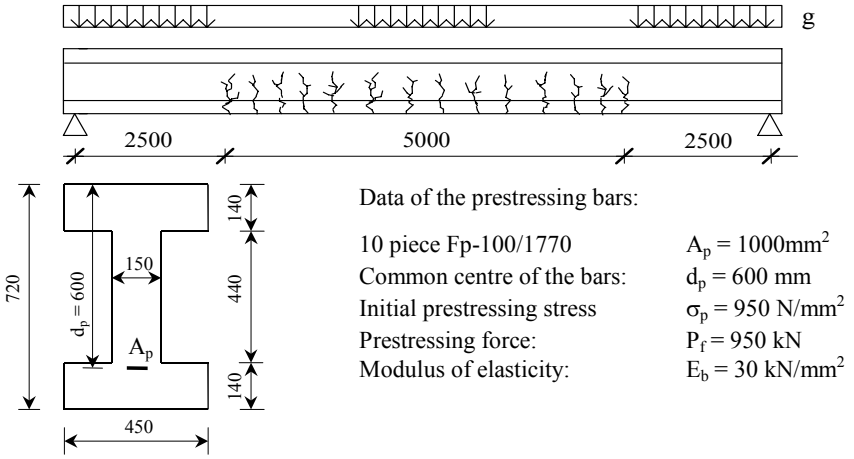

Fig. 5 Longitudinal and cross-section of the prestressed beam

For discretising in the axial direction the difference method was used again. The beam model (Fig. 5) was divided in 40 equal parts in the longitudinal direction. For the description of the D' Alembert equilibrium of the beam the (4) and (5) difference operators were used.

2.2.1 Linear and non-linear modelling of the vibration

The beam is carrying a uniformly distributed load of $g = 45$ kN/m including the self weight. This together with the effective tension force $P_f = 950$ kN makes cracks open in the middle part of the beam. Considering an undamped free vibration, three calculations were performed:

a) The first linear calculation was done with neglecting the cracks, using a constant $E_b I_{iI}$ bending stiffness along the beam.
b) The second linear calculation was performed on the cracked beam without considering the dynamic moment. The bending stiffness was constant in time, and was determined with the method in Chapter 2.1. First, the moment of inertia of curvature was developed as function of the eccentricity of the P resultant force. The Fig. 6 shows that the bending stiffness of the prestressed beam is changing gradually between the extreme values EI_{iI} and EI_{iII}.

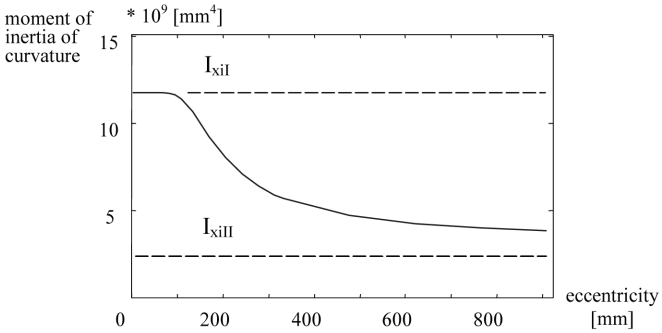

Fig. 6 Moment of inertia of curvature in function of the eccentricity of the normal force

After this, using the effective prestressing force and the static moment due to the dead load $g = 45$ kN/m, the moment of inertia of curvature was calculated from Eq. (13) in each point of the discretised beam model. Using the function in Fig. 6, the distribution of the I_g bending stiffness along the beam was obtained (Fig. 7).

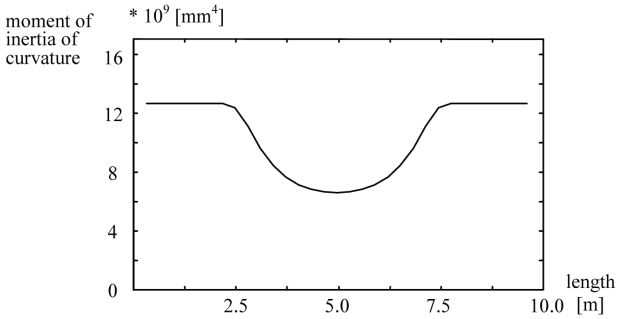

Fig. 7 Variation of the moment of inertia of curvature

c) The third solution was obtained from a non-linear calculation. The non-linearity follows from taking the dynamic moment into consideration. The eccentricity of the P resultant force was determined from the sum of the static and dynamic

moment. In this way through the eccentricity the bending stiffness of the beam is changing in time as well. The procedure was built into the Wilson's time step integral of (6). The virtual eigenfrequencies of this quasi-periodical motion were determined by discrete Fourier transformation.

Table 2 Virtual eigenfrequencies calculated with the linear and non-linear model

Calculation methods	ω_1 [Hz]	ω_2 [Hz]	ω_3 [Hz]
Linear calculation "a"	28.3	118.0	253.2
Linear calculation "b"	22.7	102.6	227.8
Non-linear calculation "c"	22.5	101.7	225.8

The eigenfrequencies calculated for the beam in Fig. 5 are compared in Table 2. It shows that the eigenfrequencies in the non-linear "c" calculation differ only slightly from that of the linear "b" solution using the static bending stiffness constant in time. This conformity is the consequence of the continuity of the bending stiffness curve (Fig. 7).

2.2.2 Linear calculation of the virtual eigenfrequencies with decreasing prestressing force

In the next step the eigenfrequencies of the beam in Fig. 5 was examined under a constant static load of $g = 31$ kN/m. The cracks just close under this load. Now suppose that the original effective prestressing force $P_f = 950$ kN is decreasing gradually, for example due to corrosion. The beam is brought into vibration. If the vibration's amplitude were small, the eigenfrequencies of the beam can be calculated with adequate accuracy, using the "b" linear method. The virtual eigenfrequencies in function of the prestressing force are listed in Table 3.

Table 3 Eigenfrequencies with different prestressing forces

Prestressing force	ω_1 [Hz]	ω_2 [Hz]	ω_3 [Hz]
1.00 P_f	34.1	136.1	305.0
0.90 P_f	33.7	135.9	302.6
0.80 P_f	31.5	133.4	291.0
0.70 P_f	27.7	124.9	276.1
0.60 P_f	24.3	113.2	260.9
0.50 P_f	21.8	103.2	247.2

In case of the full P_f prestressing force the eigenfrequencies of the girder are equal with that of the uncracked beam, because the cracks are closed. These differ from the "a" line of Table 2, because in this example (Chapter 2.2.2) the vibrating mass is smaller ($g = 31$ kN/m). According to Table 3 the eigenfrequencies decrease with the prestressing force but it becomes perceptible only below the force $0.90*P_f$. Decreasing of the eigenfrequency is best visible in the first mode.

2.3 Conclusion

In Chapter 2, the connection between the prestressing force and the virtual eigenfrequencies of the cracked prestressed beam was investigated by numeric simulation.

The virtual eigenfrequencies can be calculated with an adequate accuracy, using a linear algorithm in which the bending stiffness is constant in time. According to Table 2 the results of the linear calculation "b" differs only slightly from that of the non-linear method "c". This approximation can be applied for larger prestressed beams or bridges where the dead loads are considerably larger than the dynamic loads. Table 3 contains the virtual eigenfrequencies of the beam in function of the prestressing force.

With the aid of the above simplified linear method the curve of the eigenfrequency of the cracked, prestressed reinforced concrete beam can be plotted against the prestressing force. The diagram could also be used for temporary inspection of prestressed bridges.

REFERENCES

1. Nguyen, V. C. Experimental investigation of bending vibration of beams, Ph.D. Theses Budapest, 1994.
2. Clough R.W. and Penzien, J. Dynamics of Structure. Mc Graw-Hill Book Company, New York, 1975.
3. Pfaffinger D. D. Tragwerksdynamik, Springer Verlag, Wien, New York, 1988.
4. Bathe K.J. and Wilson E.L. Numerical Methods in Finite Element Analysis, Prentice Hall, Inc., Englewood Cliffs, N. J., 1976.
5. Korn G. A. and Korn T. M. Mathematical Handbook for Engineers, (in Hungarian), Műszaki Könyvkiadó, Budapest, 1975.
6. Dulácska E.: A rugalmas vasbetonrúd kihajlása. Építés- és Építészettudomány, 1978. X.
7. 1-2 pp. 45-65.

VIBRACIJE ARMIRANOBETONSKIH I PRETHODNONAPREGNUTIH GREDA SA PRSLINAMA

Zsolt Huszár

Prsline nastale usled prethodnog opterećenja imaju značajan uticaj na dinamičko ponašanje savijenih armiranobetonskih greda u elastičnoj oblasti. S obzirom na tu činjenicu, postoje više tačnih proračuna za sopstvene frekvencije grede. Eksperimentom se pokazuje da se vibracije razlikuju od dobro poznatog modela, ako postoji zona prslina. Uzrok ovog fenomena leži u tome da krutost na savijanje preseka u zoni prslina, zavisi od

znaka momenta svijanja. Stoga vibracije takođepokazuju nelinearnu karakteristiku u elastičnoj oblasti. Dinamičko ponašanje savijenih prethodnonapregnutih greda je slično. Osim uticaja prslina na dinamičke karakteristike prethodnonapregnutih greda, postoje još i uticaj inteziteta opterećenja i ekscentričnost aksijalne sile.

U cilju detaljnijeg istraživanja problema urađen je eksperiment i nelinearna analiza. Na njihovoj osnovi je određena virtualna sopstvena frekvencija nelinearnih vibracija.